

Capacitance-voltage profile in a structure with negative differential capacitance caused by the presence of InAs/GaAs self-assembled quantum dots

A. J. Chiquito,* Yu. A. Pusep, S. Mergulhão, and J. C. Galzerani

Departamento de Física, Universidade Federal de São Carlos, CP 676, 13565-905, São Carlos, São Paulo, Brazil

N. T. Moshegov[†]

Instituto de Física de São Carlos, Universidade de São Paulo, 13650-970, São Carlos, São Paulo, Brazil

(Received 27 April 1999; revised manuscript received 30 June 1999)

The application of the usual expressions to calculate the capacitance-voltage (CV) profiles in samples with quantum dots gives erroneous results, mainly due to the presence of the characteristic negative differential capacitance of a system with dimensionality lower than 2. We developed a simple electrostatic model to calculate the CV profiles in these systems, and we applied it to a sample with an InAs self-assembled quantum dots system in order to obtain informations about the structure of the dots. As a result, the local distribution of electrons in the quantum dots (CV profile) was obtained.

I. INTRODUCTION

It is well known that the capacitance measurements in a semiconductor heterostructure show some particular characteristics that are related to the carriers confinement.¹⁻³ In this way, the analysis of the capacitance is a very powerful technique that can be used in order to obtain the concentration and distribution of carriers, band offsets,³ density of states⁴ and other structural and electronic parameters of the semiconductors. In homogeneously doped bulk semiconductor the capacitance determines the doping concentration (N_{CV}) as a function of the distance (w) from the semiconductor surface, as established by the following equations:

$$N_{CV}(w) = \frac{C^3}{qS\epsilon_s} \left(\frac{dC}{dV} \right)^{-1} \quad (1)$$

$$w = \frac{\epsilon_s}{C} S, \quad (2)$$

where C is the system capacitance, S is the device area, and the other symbols have their usual meanings. The above equations characterize the capacitance voltage (CV) profile, giving the density of carriers along the direction of the applied electric field. As pointed out by Kreher⁵ the above equations are based on the well-defined local relation between electric potential (solution of the Poisson's equation) and the carrier's statistics. In other words, this means that the space charge region (depletion region) is gradually depleted as a function of the applied voltage: at each voltage step, a number of carriers gets out of the depletion region yielding a variation of the total charge in the semiconductor, which is measured by the capacitance. If the doping concentration profile is not constant, the N_{CV} does not reflect directly the doping distribution, but rather the carrier distribution as shown by Johnson and Panousis.⁶ Therefore, the measured capacitance is naturally limited by the screening length of the electronic system (Debye screening in a nondegenerate semiconductor or Thomas-Fermi screening in a degenerate case).

In the systems with band-gap variations such as heterostructures, where quantum effects must be considered, the capacitance is caused by two distinct contributions: a three-dimensional capacitance due to the electronic distribution in the volume around the quantum region and the capacitance due to the quantum confined electrons. When we measure the capacitance of these structures, the fundamental concept (for the bulk) of the gradual depletion of the space-charge region caused by the variation of the applied bias is not valid because the confined electronic gas moves as a whole system, changing its shape and density. More generally, the quantum contribution to the total capacitance is a direct consequence of the characteristic density of states and its occupation at a given temperature.

The above description is general and it can be used in order to describe the capacitance behavior for any structure with quantum confinement. However, the use of Eqs. (1) and (2) in these systems is only possible if the contribution of the regions with charge confinement is smaller than the contribution of the surrounding regions, because the equations which determine the CV profile were obtained for bulk structures.

In this work, our attention was focused in a structure with self-assembled InAs quantum dots producing a zero-dimensional confinement, where quantum effects are clearly observed. In this case, the direct application of Eqs. (1) and (2) is not indicated because the contribution of the quantum dots dominates. The presence of the zero-dimensional electron confinement is evidenced at low temperatures (when $e^2/C_{dots} \gg kT$, where C_{dots} is the self-capacitance of the dots) by the peculiar characteristics of the capacitance-voltage curves, such as the negative differential capacitance. As it was mentioned above, neither the spatial localization (along the growth axis) of the confined charges, nor other structural parameter which characterize the electronic distribution can be obtained by the conventional CV profile method in the quantum dots system. Thus, we present a simple electrostatic approximation based on the solution of the Poisson equation and the superposition principle in order to obtain the CV profile even in the presence of the negative

differential capacitance. More detailed aspects are given in the next section where we describe the model and the structure of the studied samples. In Sec. III, we will discuss the obtained results.

II. SAMPLE STRUCTURE AND METHOD

A. Samples

The samples used in this study were grown in a MECA 2000 molecular-beam epitaxy system on a (100) GaAs highly doped substrate; the structure is based in a plane containing InAs self-assembled dots embedded in a metal-insulator-semiconductor-field-effect-transistor (MISFET) device similar to the one proposed and used in Ref. 4. After an oxide desorption, a 100-nm-thick GaAs buffer layer doped with Si was grown at $T=580^\circ\text{C}$; then, ten periods of a Si-doped $(\text{GaAs})_{10}(\text{AlAs})_5$ superlattice were deposited followed by a $d=25$ nm undoped GaAs layer (tunneling barrier). The substrate temperature was reduced to 450°C and the InAs layer with a nominal thickness 2.3 ML was grown. The process of the dots formation was monitored by reflection high-energy electron diffraction (RHEED) oscillations: the transition from a streaked to a spotty RHEED pattern, indicating the formation of three-dimensional islands, was observed after the deposition of 1.8-ML-thick InAs. The growth was interrupted for 30 sec after the deposition of the nominal thickness of InAs. Then, an undoped GaAs separating layer (25 nm) was grown at $T=580^\circ\text{C}$ followed by an undoped GaAs/AlAs (1 nm/3 nm, $d_{SL}=120$ nm) superlattice. This superlattice was included in order to increase the sample impedance and thus, to allow us to extend the voltage range applied to the sample. Finally, the structure was capped with a 5 nm GaAs layer grown at 580°C to prevent surface oxidation. During the growth, the fluxes of InAs and GaAs were fixed at 0.1 and 0.35 ML/s respectively, while $P_{As}=5\times 10^{-6}$ Pa. The total thickness of the samples was $t=175$ nm. For the Schottky diode construction, we fabricated a conventional Ohmic contact on the substrate with an AuGeNi alloy annealed at 450°C for 120 s; the Schottky contact was formed by the deposition of a 200 nm aluminum layer with $500\ \mu\text{m}$ diameter. Figure 1 shows a sketch of the conduction band bottom of our samples with a bias applied to the Schottky contact.

The capacitance-voltage curves were obtained from admittance measurements that were carried out using a standard lock-in technique (with a SR530 Stanford lock-in amplifier). The samples were mounted in a variable temperature cryostat coupled with the measurement system; the CV curves were measured at a fixed frequency ($f=100$ kHz) in the temperature range from 8 to 300 K.

Before the Schottky diode construction, photoluminescence (PL) measurements were carried out at $T=17$ K. The corresponding photoluminescence spectrum is shown in Fig. 2. The PL spectrum shows two peaks: the electron-hole recombination in the InAs dots is responsible for the peak at $E=1.24$ eV with a $\Delta E=111.2$ meV energy broadening as obtained by a Gaussian fit. The energy $E=1.24$ eV corresponds to an electron level located at 80 meV below the conduction band of GaAs as it was calculated using the discontinuity energy for the conduction band $\Delta E_{CB}=0.85\times(E_{\text{GaAs}}-E_{\text{InAs}})$. The other peak at $E=1.51$ eV is associ-

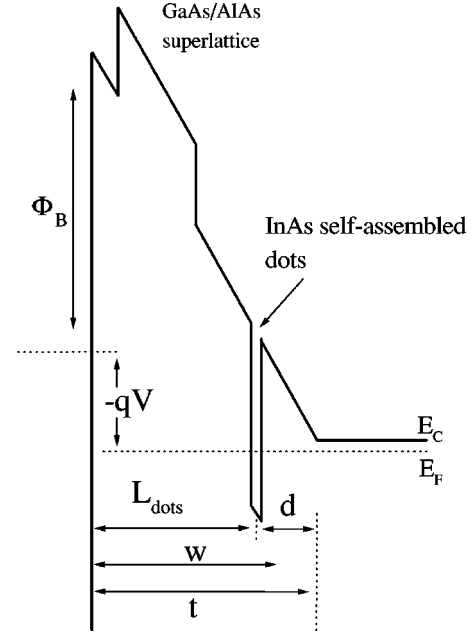


FIG. 1. Bottom of the conduction band for the InAs/GaAs self-assembled quantum dots used in this work. L_{dots} is the position of the layers with quantum dots and w is the width of the depletion region.

ated with the luminescence of the bulk GaAs. The broadening energy value determined in our PL measurements is in accordance with the previously reported values of this parameter.^{7,8}

The capacitance-voltage curve of the structure under investigation measured at $T=8$ K is plotted in the inset of Fig.

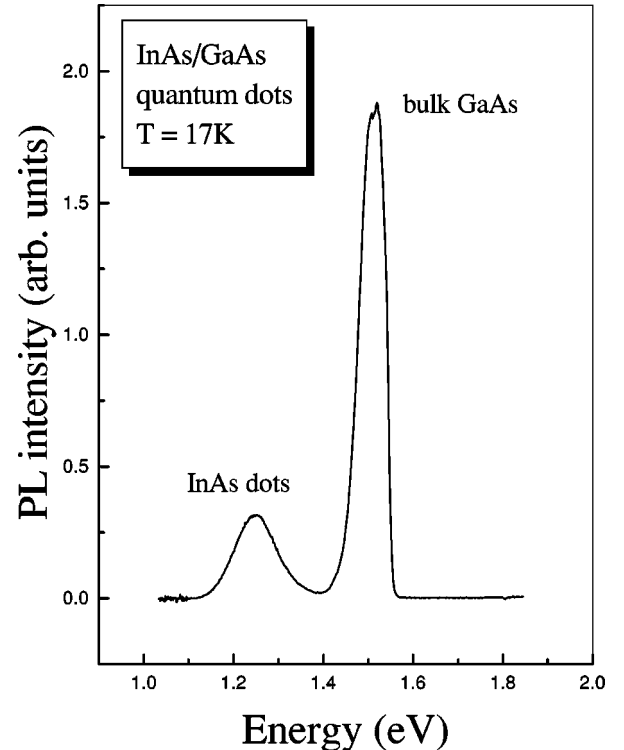


FIG. 2. PL spectrum obtained for the sample with InAs dots at $T=17$ K, which is characterized by the value of the energy dispersion equal to 111.2 meV.

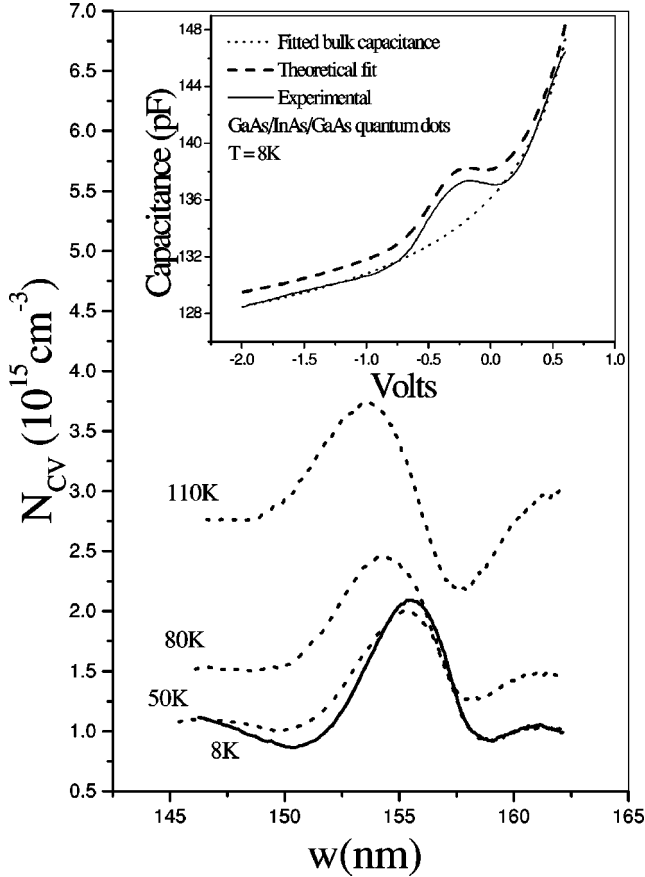


FIG. 3. The CV profiles calculated at different temperatures using Eq. (14). The positions for the electron concentration maxima represent the positions of the plane of dots which are found in good agreement with the corresponding nominal position. The inset shows the experimental capacitance-voltage characteristics for our sample with InAs dots (full line). The negative differential capacitance between -0.8 and 0.2 V is an evidence of the zero-dimensional character of the quantum dots. The dotted line curve are the bulk background fit taken in order to extract the capacitive effects of the quantum dots. The dashed line is the calculated capacitance shifted up for clearness.

3. Two contributions can be distinguished: the background capacitance (showed by the dotted line) and the superimposed capacitance of the dots revealed in the peak at $V = -0.15$ V. The following equation was used to obtain the GaAs bulk contribution which is dominant in the $V < -1$ V and $V > 0.2$ V voltage range (see the inset of Fig. 3):

$$C = C_0 + S \sqrt{\frac{qN_{CV}\epsilon}{2(\phi_B - V)}}, \quad (3)$$

where N_{CV} is the donors concentration, S is the Schottky contact area and the other parameters have their usual meanings. Thus, the adjusted values of these quantities were obtained: $\phi_B = 0.96$ eV and $N_{CV} = 7.8 \times 10^{14}$ cm $^{-3}$. C_0 is the contribution of the GaAs/AlAs superlattice and it is inversely proportional to the superlattice thickness. The fitting of the Eq. (3) to the background of the experimental capacitance-voltage curve (shown by the dotted line in the inset of Fig. 3)

yields $C_0 = 120$ pF, in agreement with the calculated value $C_0 \approx \epsilon S/d_{SL} = 170$ pF (where ϵ was taken as the dielectric constant of GaAs).

B. Dots capacitance model

In the voltage range from -1.0 to 0.2 V, the main contribution to the total capacitance is due to the InAs self-assembled quantum dots and it reflects their zero-dimensional density of states (inset of Fig. 3); the behavior of the capacitance in this voltage range can be explained as follows: starting at $V = -0.8$ V, the measured capacitance increases due to the filling of the dots, showing a peak at $V = -0.15$ V (the peak is broad due to fluctuations in their sizes); if the voltage increases, the capacitance signal diminishes because the dots are completely filled and for a further increase of the applied voltage, the total capacitance is given by the contribution of the bulk GaAs. The charge located in the InAs quantum dots depends on the voltage, temperature and density of states. In order to calculate the capacitance of our samples we used a simple model based on the definition of the capacitance ($C = dQ/dV$) where the charge is given by the integral of the product of the density of states and the energy distribution

$$C_{dot} = 2qSL \frac{\partial}{\partial V_{dot}} \left[\int D(\epsilon, V_{dot}) \times f(\epsilon, V_{dot}) d\epsilon \right], \quad (4)$$

with

$$D(\epsilon, V_{dot}) = \frac{N_{dot}}{\sqrt{\frac{\pi}{2} \Delta \epsilon}} \exp \left[-2 \left(\frac{\epsilon + \epsilon_{dot} + qV_{dot}}{\Delta \epsilon} \right)^2 \right] \quad (4a)$$

$$f(\epsilon, V_{dot}) = \frac{1}{1 + \exp \left[\frac{q(\epsilon - qV_{dot})}{kT} \right]}, \quad (4b)$$

where $D(\epsilon, V_{dot})$ is the electron density of states, $f(\epsilon, V_{dot})$ is the Fermi-Dirac energy distribution, V_{dot} is the voltage across the quantum dots scaled by a lever-arm relation when the band bending is neglected.⁹ The factor 2 in Eq. (4) reflects the electron spin, S is the contact area and L is the lever arm coefficient ($L = d/t$, d is the tunneling barrier thickness and t is the total sample thickness; therefore, $L = 7$ for the samples used in this work). ϵ_{dot} is the confined energy level in the quantum dots with respect to the GaAs conduction band, $\Delta \epsilon$ is the energy dispersion and N_{dot} is the total number of dots. The density of states in the InAs dots can be written in a delta function form in the ideal case (no dots size dispersion); here, we must include the effects of the dots size dispersion by taking into account a Gaussian broadening of the density of states as it is shown in Eq. (4a).¹⁰ For the calculations, only the occupied states were considered and we assumed that the Fermi level in the dots was the same as in the highly doped substrate.¹¹ Then, the Eq. (4) was numerically solved with ϵ_{dot} , $\Delta \epsilon$ and N_{dot} used as fitting parameters; the calculated capacitance is shown in the inset of Fig. 3.

The obtained values for the confined level energy ($\varepsilon_{dot} = 79$ meV) and for the energy dispersion ($\Delta\varepsilon = 113$ meV) were found in excellent accordance with the photoluminescence measurements; in addition, the value $N_{dot} = 6.5 \times 10^{10} \text{ cm}^{-2}$ was found. As it is well established, the magnitude of the energy dispersion of electronic states is directly related to the width of the PL spectrum.^{2,12} It should be mentioned that the characteristic parameters of the dots can be obtained by a solution of the Poisson's equation for the entire structure, as it has been done in Ref. 12. However, as it will be shown in the next section, our analysis allows determine the CV profile as well, and thus, to obtain the structural parameters of the quantum dots (such as the spatial distribution of electrons and dots height) in addition to the energetical parameters.

C. CV profile calculation

The voltage interval where the negative differential capacitance occurs in our samples is clearly seen in the inset of Fig. 3. In this case, as it was mentioned above, the CV profile [Eqs. (1) and (2)] cannot be applied to the experimental curves. Equation (1) essentially means that the electronic distribution in a given (bulk) structure can be written as a function of the measured capacitance. Therefore, an alternative and direct method for the construction of the CV profile in our samples is the calculation of a general expression for the spatial electronic distribution along the structure as a function of the total capacitance

$$N_{CV}(w) = F(C_{total}) \equiv F(w) \quad (5)$$

with

$$C_{total} = G(C_{bulk}, C_{dots}), \quad (6)$$

where w is the depletion region, F and G are unknown functions. The formal dependence established by Eq. (5) is only possible to obtain if there is a well defined relation between the capacitance and the depletion width. In a quantum dots system, this relation cannot be determined because the depletion approximation is not valid for a system with dimensionality lower than 3 as mentioned in the introduction. As an additional complication, the total capacitance C_{total} is an unknown function of both the bulk and dots capacitances as shown in Eq. (5). In other words, an expression that gives the relation between the electron distribution and the capacitance like Eq. (1) is not possible to be achieved for a system containing quantum dots. Therefore, we present some considerations based in the electrostatic Poisson equation and in the superposition principle that allows to calculate an approximate equation for the determination of the spatial electronic distribution as a function of the capacitance (or the distance from the semiconductor surface). This task involves the determination of the functions F and G , which were calculated using a particular coupling between the capacitances C_{bulk} and C_{dots} .

In order to calculate the CV profile of the structure studied here we need to consider the sources of the charges contributing to the capacitance: the net charge is given by the free three-dimensional electrons in the GaAs surrounding the dots (unintentional background doping) and by the confined electrons in the dots, which are regarded as punctual charges

(we assume no particular interaction between the dots). Then, the density of charge is given by the following expression:¹³

$$\rho(z) = q \left[N_{CV} w - \int D(\varepsilon, V_{dot}) \times f(\varepsilon, V_{dot}) d\varepsilon \right]. \quad (7)$$

The integration of the Poisson equation from the surface to the interior of the semiconductor can be written as

$$V - \Phi_B = \frac{-q N_{CV} w^2}{2\varepsilon_s} + \frac{q L_{dots}}{\varepsilon_s} \int D(\varepsilon, V_{dot}) \times f(\varepsilon, V_{dot}) d\varepsilon, \quad (8)$$

where Φ_B and N_{CV} are the Schottky barrier height and the density of charges in the depletion region, respectively. The quantities L_{dots} and w are shown in Fig. 1: L_{dots} is the nominal position of the dots plane measured from the semiconductor surface and w is the width of the depletion layer. The last term of Eq. (8) is the electronic density of the plane containing the dots (represented by a quantum well in Fig. 1). Note that in this model we consider the bulk and the quantum dots contributions as noninteracting ones. The differentiation of Eq. (8) with respect to the bias can be written as

$$\Delta V = -q N_{CV} w \left[\frac{-\varepsilon_s}{C_{bulk}^2} \Delta C_{bulk} \right] + \frac{q L_{dots}}{\varepsilon_s} \Delta n, \quad (9)$$

with

$$\Delta n = \frac{d}{dV} \left[\int D(\varepsilon, V_{dot}) \times f(\varepsilon, V_{dot}) d\varepsilon \right] dV. \quad (10)$$

Equation (10) shows the charge variation in the dots plane, which produces the dots contribution to the total capacitance in all range of voltages. In order to derive Eq. (9) we used the total capacitance written in an approximate form (parallel plates capacitance) as it is usually done in bulk structures. Rearranging the terms, we obtain

$$N_{CV} = \frac{C_{bulk}^3}{q\varepsilon_s} \left(\frac{dC_{bulk}}{dV} \right)^{-1} \left[1 + \frac{q L_{dots}}{\varepsilon_s} \frac{\Delta n}{\Delta V} \right], \quad (11)$$

with

$$w = \frac{\varepsilon_s}{C_{bulk}} S, \quad (12)$$

where C_{bulk} is the capacitance of the bulk structure without quantum dots.

The above Eqs. (7)–(12) describe the dots as a pure electrostatic system embedded in a bulk structure in agreement with the chosen parallel coupling for the dots and bulk capacitances.¹¹ The established dependence between the distribution of electrons and capacitance allows us to determine the form of function F , as follows from Eq. (11). Using Eq. (5), Eq. (11) can be rewritten as

$$N_{CV} = F_1(C_{bulk}) + F_2(C_{dots}), \quad (13)$$

where

$$F_1(C_{bulk}) = \frac{C_{bulk}^3}{q\epsilon_s} \left(\frac{dC_{bulk}}{dV} \right)^{-1} \quad (14)$$

$$F_2(C_{dots}) = \left[\frac{C_{bulk}^3}{q\epsilon_s} \left(\frac{dC_{bulk}}{dV} \right)^{-1} \right] \times \left[\frac{qL_{dots}}{\epsilon_s} \frac{\Delta n}{\Delta V} \right]. \quad (15)$$

This means that the unknown dependence of the confined electrons upon the width of the depletion region is determined by the product indicated in function $F_2(C_{dots})$ above. The dependence of the function $F_2(C_{dots})$ on the nominal position of the dots plane (L_{dots}) give an uncertainty in the amplitude of the CV profile. It is worthwhile to notice two points: firstly, we consider a linear form for the unknown function G , which states the dependence of the total capacitance [$C_{total} = C_{bulk} + C_{dots}$,⁹ in Eq. (6)] on the bulk and dots capacitance; secondly, the dots contribution in Eq. (11) is proportional to the capacitance of the dots per unity of charge and area, and implicitly contains the dimensionality of the confined system through the density of states as established by Eq. (10).

Equations (11) and (12) relate to the electron concentrations and are consistent with the superposition principle above mentioned; additionally, they are valid for any charge distribution. The interpretation and use of these equations is as follows: the reciprocal value of the capacitance C_{bulk} determines the distance from the semiconductor surface [in analogy with Eq. (2)]; Eq. (11) includes both contributions: the bulk (constant throughout the structure) and the confined electrons in the dots plane. In order to construct the CV profile using these equations some important steps are necessary: first, both the dots and bulk contributions to the total capacitance were separated as it is presented by Eq. (13) [the dotted line in the inset of Fig. 3 represents the bulk capacitance fitted to the measured capacitance by means of Eq. (3)]. Then, the bulk contribution was used both to determine the distances from the surface [given by Eq. (12)] and to calculate the average background density of electrons. The presence of the quantum dots makes the second term in the brackets of Eq. (11) comparable to unity, giving an additional contribution to the calculated bulk profile at the dots plane, which finally was calculated according to Eqs. (11) and (13).

III. DISCUSSION

The results of the calculations based in Eqs. (11) and (12) applied to the capacitance-voltage curves are plotted in Fig. 3. A direct comparison between the assumed nominal electron distribution and the obtained results gives good accordance: the nominal position of the dots is $L_{dots} = 150$ nm from the Schottky contact and Eqs. (12) gives $z_{dots} = 155$ nm for the electron accumulation position (Fig. 3). The difference between these two values can be compared with the error due to the electron screening effects found in usual CV profiles obtained in bulk or two-dimensional structures.¹ By the other hand, the profile width does not represent the distribution of the position of dots in the plane containing them: as in a quantum well system, the full width at half maximum is related to the spatial resolution of the CV profile along the growth direction.¹⁴ Thus, we can use the

profile width in order to evaluate the effective electronic radius which can be considered as an estimative of the height of the self-assembled dots and the density of electrons localized in the dots. We have found an average value of 5 nm for the CV profile width (effective electron radius), in agreement with the height of the self-assembled quantum dots presented in literature.^{15,16} The density of electrons in the plane containing the dots can be obtained from the CV profile by the integration of the $N_{CV} \times w$ curves.¹⁷ Using this procedure with the curves plotted in Fig. 3 we obtained an average value of the density of electrons in the quantum dots region equal to $n \approx 5 \times 10^9 \text{ cm}^{-2}$.

It is worse adding that the peak of the capacitance presented in the inset of Fig. 3 disappears with the increase of temperature. In addition, the calculation of the CV profiles done for different temperatures showed the systematic shift of the peak position toward the surface with the increase of temperature, which can be caused by the dynamical process involving the capture/emission rates of the dots. As it was shown in Ref. 10, if the rate of thermal emission of electrons from the quantum dots is smaller than the frequency of the ac signal (used in the capacitance measurement), there will be no response to this ac excitation; at low temperatures the capacitance is mainly due to the electrons through the triangular barrier behind the dots. Thus, at these temperatures a small shift appears on the CV profile position because a higher electric field is necessary for the tunneling process to occur. At higher temperatures, when the thermal emission becomes important, there is no such shift and the CV profile was found to be closer to the nominal position of the dots plane. This process describes well the experimental behavior observed in our samples and it is an evidence that the measured capacitance at low temperatures is caused by the electron tunneling from the dots to the highly doped substrate. Moreover, the variation of the maximum intensity of the CV profiles at different temperatures (showed in Fig. 3) confirms that at high temperatures an additional quantity of electrons contribute (probably due to the thermal excitation of the bulk electrons), increasing the measured capacitance and, as a consequence, the intensity of the CV profiles.

Finally, the supposition about a linear coupling between the capacitances due to the dots and to the bulk plays a fundamental role in our model: as mentioned in Sec. II, in order to calculate the CV profile it is necessary to know the function linking the electronic distribution to the total capacitance of the structure. We can consider that the whole system behaves like a parallel coupling of two capacitors, where the measured capacitance contains distinguishable parts, which are individually related to the bulk and dots contributions. Actually, in a more general treatment for the equivalent circuit we should consider other electrical components for the model and probably other types of coupling between these components. However, the validity of the superposition of the capacitances used for the samples here studied was confirmed by the agreement between the nominal and calculated values of the dots plane position.

To conclude, it was shown that the presence of a differential capacitance is an indicator of an electronic system with a dimensionality smaller than 2. In this case, the conventional method of calculation of the CV profile used for the bulk is not valid and therefore, we developed a simple method to obtain structural parameters of the self-assembled

quantum dots by means of the capacitance-voltage measurements. As a result, the structural parameters of the dots such as the position of the plane containing dots, the dots density, the concentration of electrons occupying the dots and an estimate of the dots height were obtained.

ACKNOWLEDGMENTS

The authors wish to thank E. Diagonal for his help in samples processing and Brazilian agencies CNPq and FAPESP for financial support.

*Electronic address: pajc@power.ufscar.br

†On leave from the Institute of Semiconductors Physics, 630090, Novosibirsk, Russia.

¹E.F. Schubert, *Doping in III-V Semiconductors* (Cambridge University Press, Cambridge, England, 1993).

²P.N. Brunkov, T. Beniyattou, and G. Guillot, *J. Appl. Phys.* **80**, 864 (1996).

³H. Kroemer, W.Y. Chien, J.S. Harris, Jr., and D.D. Edwall, *Appl. Phys. Lett.* **36**, 295 (1980).

⁴G. Medeiros-Ribeiro, D. Leonard, and P.M. Petroff, *Appl. Phys. Lett.* **66**, 1767 (1995); G. Medeiros-Ribeiro, Ph.D. dissertation, Universidade Federal de Minas Gerais, 1996.

⁵K. Kreher, *Phys. Status Solidi A* **135**, 597 (1993).

⁶W.C. Johnson and P.T. Panousis, *IEEE Trans. Electron Devices* **18**, 965 (1971).

⁷K.H. Schmidt, G. Medeiros-Ribeiro, M. Oestreich, P.M. Petroff, and G.H. Döhler, *Phys. Rev. B* **54**, 11 346 (1996).

⁸K.H. Schmidt, G. Medeiros-Ribeiro, and P.M. Petroff, *Phys. Rev. B* **58**, 3597 (1998).

⁹G. Medeiros-Ribeiro, F.G. Pikus, P.M. Petroff, and A.L. Efros, *Phys. Rev. B* **55**, 1568 (1997).

¹⁰P.N. Brunkov, A.A. Suvorova, N.A. Bert, A.R. Kovsh, A.E. Zhukov, A.Yu. Egorov, V.M. Ustinov, A.F. Tsatsulnikov, N.N. Ledentsov, P.S. Kopev, S.G. Konnikov, L. Eaves and P.S. Main, *Semiconductors* **32**, 1096 (1998).

¹¹Ph. Lelong, O. Heller, and G. Bastard, *Physica E* **2**, 678 (1998).

¹²P.N. Brunkov, A. Polimeni, S.T. Stoddart, M. Henini, L. Eaves, P.C. Main, A.R. Kovsh, Yu.G. Musikhin, and S.G. Konnikov, *Appl. Phys. Lett.* **73**, 1092 (1998).

¹³J.M. Lopez-Villegas, P. Roura, J. Bosch, J.R. Morante, A. Georgakilas, and K. Zekentes, *J. Electrochem. Soc.* **140**, 1492 (1993).

¹⁴E.F. Schubert, R.F. Kopf, J.M. Kuo, H.S. Luftman, and P.A. Garbinski, *Appl. Phys. Lett.* **57**, 497 (1990).

¹⁵M. Grundmann, O. Stier, and D. Bimberg, *Phys. Rev. B* **52**, 11 969 (1995).

¹⁶M. Grundmann, J. Christen, N.N. Ledentsov, J. Bóhrer, D. Bimberg, S.S. Ruvimov, P. Werner, U. Richter, U. Gösele, J. Heydenreich, V.M. Ustinov, A.Yu. Egorov, A.E. Zhukov, P.S. Kopev, and Zh.I. Alferov, *Phys. Rev. Lett.* **74**, 4043 (1995).

¹⁷E.F. Schubert, in *Semiconductors and Semimetals* (Academic Press, New York, 1994), Vol. 40, Chap. 1.